

Non-Abelian momentum polytopes for products of \mathbb{CP}^2

James Montaldi & Amna Shaddad

University of Manchester

Dedicated to Darryl Holm on the occasion of his 70th birthday

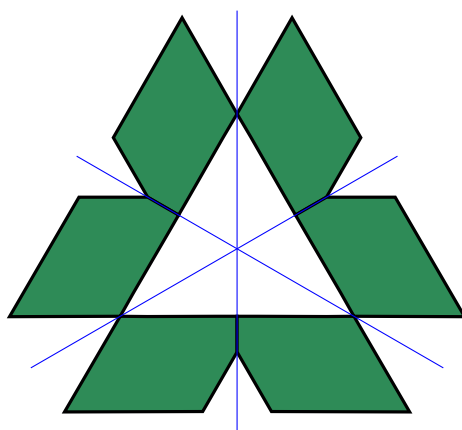
Abstract

This is the first of two companion papers. The joint aim is to study a generalization to higher dimension of the point vortex systems familiar in 2-D. In this paper we classify the momentum polytopes for the action of the Lie group $SU(3)$ on products of copies of complex projective 4-space. For 2 copies, the momentum polytope is simply a line segment, which can sit in the positive Weyl chamber in a small number of ways. For a product of 3 copies there are 8 different types of generic momentum polytope, and numerous transition polytopes, all of which are classified here. The type of polytope depends on the weights of the symplectic form on each copy of projective space. In the second paper we use techniques of symplectic reduction to study the possible dynamics of interacting generalized point vortices.

The results can be applied to determine the inequalities satisfied by the eigenvalues of the sum of up to three 3×3 Hermitian matrices with double eigenvalues.

MSC 2010: 53D20

Keywords: Momentum map, convex polyhedra, symplectic geometry, eigenvalue estimates



Contents

1	Introduction	2
2	Hamiltonian action of $SU(3)$ on products of projective spaces	4
2.1	Background	4
2.2	Momentum map for the $SU(3)$ action on products of \mathbb{CP}^2	9
2.3	Coadjoint orbits	11
2.4	Action of $SU(3)$ on products of \mathbb{CP}^2	12
3	Momentum polytopes for $SU(3)$ action on $\mathbb{CP}^2 \times \mathbb{CP}^2$	13
4	Momentum polytopes for $SU(3)$ action on $\mathbb{CP}^2 \times \mathbb{CP}^2 \times \mathbb{CP}^2$	15
4.1	Generic polytopes	19
4.2	Transition polytopes	24
	References	27

1 Introduction

The now famous convexity theorem of Atiyah, Guillemin and Sternberg and finally Kirwan for the momentum polytope has an interesting history.

In the 1920s, Schur [13] proved that the diagonal elements $(\delta_1, \dots, \delta_n)$ of an $n \times n$ Hermitian matrix A satisfy a system of linear inequalities involving the eigenvalues $(\lambda_1, \dots, \lambda_n)$. In geometric terms, regarding δ and λ as points in \mathbb{R}^n and allowing the symmetric group S_n to act by permutation of coordinates, this result says that δ lies in the convex hull of the orbit $S_n \cdot \lambda$.

The converse was proved in the 1950s by Horn [5], and thus this convex hull is exactly the set of diagonals of the set of all Hermitian matrices with given eigenvalues $(\lambda_1, \dots, \lambda_n)$.

Kostant generalised these results to any compact Lie group G in the following manner [8]. Consider the coadjoint action of G on the dual \mathfrak{g}^* of its Lie algebra \mathfrak{g} . Let $\mathbb{T} \subseteq G$ be a maximal torus, with Lie algebra \mathfrak{t} . Restriction to \mathfrak{t} defines a projection $\mathfrak{g}^* \rightarrow \mathfrak{t}^*$. The Weyl group W acts on \mathfrak{t} and \mathfrak{t}^* . Kostant's convexity theorem states,

Let $\mathcal{O} \subseteq \mathfrak{g}^$ be a coadjoint orbit under G . Then the projection of \mathcal{O} on \mathfrak{t}^* is the convex hull of a Weyl group orbit.*

The Schur-Horn theorem is the particular case where G is the unitary group $U(n)$ and \mathbb{T} is the subgroup of diagonal matrices. Then \mathfrak{g} is the Lie algebra of skew-Hermitian matrices. The dual \mathfrak{g}^* can be identified with the set of Hermitian matrices via the pairing $\langle A, B \rangle := \text{Im tr}(AB)$,

The picture on the front cover is the intersection of the image of the momentum map with the dual of the Cartan subalgebra, for symplectic weights of type H (see Fig. 4.1): it does not appear in the published version.

for A Hermitian and B skew-Hermitian. Then the projection of $A \in \mathfrak{g}^*$ on \mathfrak{t}^* is given by the diagonal part of A .

This convexity theorem was widely generalised (Atiyah [1], Guillemin-Sternberg [3], Kirwan [6], etc.). The general relevant framework is that of a symplectic manifold M with a Hamiltonian action of a Lie group G . The projection $\mathcal{O} \rightarrow \mathfrak{t}^*$ is a particular case of a momentum map, $M \rightarrow \mathfrak{g}^*$. The most general of these theorems, due to Kirwan, states that the intersection of the image of the momentum map with a positive Weyl chamber in \mathfrak{t}^* is a convex polytope, the *momentum polytope*.

In the vein of the Schur-Horn theorem, this non-Abelian convexity theorem shows for example that if A and B are Hermitian matrices with given eigenvalues, then the eigenvalues of their sum $A + B$ are bounded by a set of linear inequalities involving the given eigenvalues of A and B . See [7] for a description of these ideas.

In this paper we consider an extended example based on the natural action of $SU(3)$ on \mathbb{CP}^2 : given $A \in SU(3)$ and $[v] \in \mathbb{CP}^2$ then $A[v] = [Av]$ (in fact the action factors through that of $\mathbb{P}SU(3)$ which is $SU(3)$ factored by the 3-element centre of $SU(3)$, but this has no effect on the material in this paper). On \mathbb{CP}^2 there is an $SU(3)$ -invariant symplectic form, the Fubini-Study form, and in fact any invariant symplectic form is a scalar multiple of this particular one. We consider the compact manifold M given by the product of 2 or 3 copies of \mathbb{CP}^2 , with the diagonal action of $SU(3)$, and on each copy we choose an invariant symplectic form, with scalars (weights) Γ_j (for $j = 1, 2, 3$). The action of $SU(3)$ on M is Hamiltonian and the momentum map depends on the choice of weights Γ_j . The aim of this work is to classify all possible momentum polytopes, depending on the weights. Note that we use the term ‘weights’ both for the coefficients Γ_j and for the weights of a representation: we hope it is clear from the context which one is meant. In the companion paper [10], the symplectic weights are called *vortex strengths*.

The paper is organized as follows. After introducing the necessary background in Section 2, Section 3 is dedicated to determining the possible momentum polytopes for the actions of $SU(3)$ on $\mathbb{CP}^2 \times \mathbb{CP}^2$, showing there are generically 2 different possible ‘shapes’; these are just line segments in the positive Weyl chamber (there are also 2 others that are reflections of the first two). In Section 4 we consider the more interesting case of $\mathbb{CP}^2 \times \mathbb{CP}^2 \times \mathbb{CP}^2$. We show that, depending on the weights Γ_j , there are generically 8 distinct types of momentum polytope as well as their reflections under the $*$ -involution; there are also numerous transition shapes as the weights vary.

This is the first of two companion papers; the second [10] uses the results of this paper to study the (reduced) dynamics of a system of generalized point vortices on \mathbb{CP}^2 , which has symmetry $SU(3)$, acting on a phase space which is the product of copies of \mathbb{CP}^2 . In that paper we discuss the reduced spaces and consider the resulting reduced dynamics and in particular the reduced and relative equilibria and their stability.

This work forms part of the PhD thesis [14], where further details and alternatives for some of the calculations may be found.

Eigenvalues of Hermitian matrices Following the line of argument of the non-Abelian version of the Schur-Horn theorem mentioned above, one application of our results is to esti-

inating the eigenvalues of the sum of up to three 3×3 Hermitian matrices, each with a double eigenvalue.

Let A, B, C be three trace-zero 3×3 Hermitian matrices each with a double eigenvalue, and let $X = A + B + C$ (if they are not trace zero then replace A by its trace-free part $A_0 = A - \frac{1}{3} \text{tr}(A) I_3$, and similarly for B and C). Denote the eigenvalues of A by $\lambda_A, \lambda_A, -2\lambda_A$, and similarly for B and C .

Theorem 1.1 (1). *If $C = 0$, then the eigenvalues λ_j of $X = A + B$, satisfy $\lambda_1 + \lambda_2 + \lambda_3 = 0$ and*

$$\lambda_1 = \lambda_A + \lambda_B, \quad \lambda_2 \in \begin{cases} [\lambda_A - 2\lambda_B, \lambda_A + \lambda_B] & \text{if } \lambda_B > 0, \\ [\lambda_A + \lambda_B, \lambda_A - 2\lambda_B] & \text{if } \lambda_B < 0. \end{cases}$$

(2). *More generally (with $A, B, C \neq 0$), the spectrum of $X = A + B + C$ lies in one of the convex polytopes shown in the figures of Section 4 or its image under the involution $*$, according to the eigenvalues of A, B, C .*

Moreover, given any triple $(\lambda_1, \lambda_2, \lambda_3)$ satisfying these inequalities there are Hermitian matrices A with eigenvalues $\lambda_A, \lambda_A, -2\lambda_A$ and B, C with similar eigenvalues, such that $\lambda_1, \lambda_2, \lambda_3$ are the eigenvalues of $A + B + C$.

For example, in part (2), if $\lambda_C = \lambda_B = \lambda_A > 0$ then the eigenvalues λ_j of X sum to zero and satisfy the inequalities (deduced from Figure 4.8b and equations (4.1)),

$$\lambda_j \leq 3\lambda_A, \quad j = 1, 2, 3.$$

Part (1) of this theorem is proved at the end of Section 3; the proof of part (2) is entirely analogous and is left to the reader.

2 Hamiltonian action of $SU(3)$ on products of projective spaces

In this section we provide the background required, regarding $SU(3)$, symplectic actions and the resulting momentum maps.

2.1 Background

Recall that if a Lie group acts on a symplectic manifold (M, Ω) then a momentum map is a map $J : M \rightarrow \mathfrak{g}^*$, where \mathfrak{g} is the Lie algebra and \mathfrak{g}^* its dual vector space, satisfying the differential condition,

$$\langle DJ_x(v), \xi \rangle = \Omega(\xi_M(x), v), \quad (2.1)$$

where ξ_M is the vector field on M associated to $\xi \in \mathfrak{g}$.

A Lie group G acts naturally on its Lie algebra \mathfrak{g} by the adjoint action and on the dual space \mathfrak{g}^* by the contragredient representation, the coadjoint action. An orbit in \mathfrak{g}^* is called a coadjoint orbit. If, as is our case, the group is compact then the adjoint and coadjoint actions are isomorphic. If, as we suppose, G is compact and there exists a momentum map, then one can be

chosen so that it is equivariant with respect to the given action on M and the coadjoint action on \mathfrak{g}^* .

If V is a symplectic representation of G , then the momentum map is given by

$$\langle J(v), \xi \rangle = \frac{1}{2} [\xi v, v], \quad (\xi \in \mathfrak{g}).$$

where $[-, -]$ is the symplectic form. An important example is the momentum map for a complex representation V of a torus \mathbb{T} . Then V is a direct sum of 1-dimensional irreducible representations, of weights β_j , $j = 1, \dots, n$ (where $\dim_{\mathbb{C}} V = n$, with possible repeats among the β_j , and possible zeros). Recall that given a complex representation V of \mathbb{T} , the form $\beta \in \mathfrak{t}^*$ is a weight if the weight-space V_β is non-zero, where

$$V_\beta = \{v \in V \mid \xi v = i\beta(\xi)v, \forall \xi \in \mathfrak{t}\}.$$

If we identify V with \mathbb{C}^n , with each coordinate axis being an irreducible representation, then the symplectic form can be written as $[u, v] = \sum_j \text{Im}(u_j \bar{v}_j)$. Then

$$J(v) = \frac{1}{2} \sum_j |v_j|^2 \beta_j \in \mathfrak{t}^*.$$

If instead the symplectic form is altered to $[u, v] = \sum_j \Gamma_j \text{Im}(u_j \bar{v}_j)$, then the momentum map becomes

$$J(v) = \frac{1}{2} \sum_j \Gamma_j |v_j|^2 \beta_j \in \mathfrak{t}^*. \quad (2.2)$$

Coadjoint orbits carry a natural symplectic structure, the Kirillov-Kostant-Souriau, or KKS 2-form, defined by

$$\omega_{\text{KKS}}(\mu)(\xi \cdot \mu, \eta \cdot \mu) := \langle \mu, [\xi, \eta] \rangle,$$

for $\mu \in \mathfrak{g}^*$ and $\xi, \eta \in \mathfrak{g}$. If \mathcal{O} is such a coadjoint orbit with its KKS-form then the coadjoint action of G on \mathcal{O} is Hamiltonian and the momentum map $J : \mathcal{O} \rightarrow \mathfrak{g}^*$ is simply given by the inclusion of \mathcal{O} into \mathfrak{g}^* (see for example [4]).

An important property of momentum maps, often called the bifurcation lemma, and that we will make considerable use of is that, for each $m \in M$,

$$\text{image}(DJ_m) = \mathfrak{g}_m^\circ, \quad (2.3)$$

where \mathfrak{g}_m is the Lie algebra of the stabilizer of the point m , and \mathfrak{g}_m° its annihilator in \mathfrak{g}^* . This follows readily from (2.1).

Given a point $\mu \in \mathfrak{g}^*$ its stabilizer subgroup for the coadjoint action is denoted G_μ . Any maximal torus \mathbb{T} of G_μ is also a maximal torus of G . At the level of Lie algebras, $\mathfrak{g}_\mu = \mathfrak{z}_\mu \times \mathfrak{g}'_\mu$, where \mathfrak{z}_μ is the centre of \mathfrak{g}_μ . Dualizing, we can write

$$\mathfrak{g}^* = \mathfrak{z}_\mu^* \times (\mathfrak{g}'_\mu)^*. \quad (2.4)$$

It follows that $\mathfrak{z}_\mu^* = \text{Fix}(G_\mu, \mathfrak{g}^*)$, and similarly we may identify \mathfrak{g}_μ^* as the subspace of \mathfrak{g}^* given by $\mathfrak{g}_\mu^* := \text{Fix}(\mathfrak{z}_\mu, \mathfrak{g}^*)$.

One particular case is the Cartan subalgebra \mathfrak{t} and its dual $\mathfrak{t}^* = \text{Fix}(\mathbb{T}, \mathfrak{g}^*)$. The Weyl group acts on \mathfrak{t}^* , and we denote a closed fundamental domain by \mathfrak{t}_+^* . For $\text{SU}(3)$, see Figure 2.1.

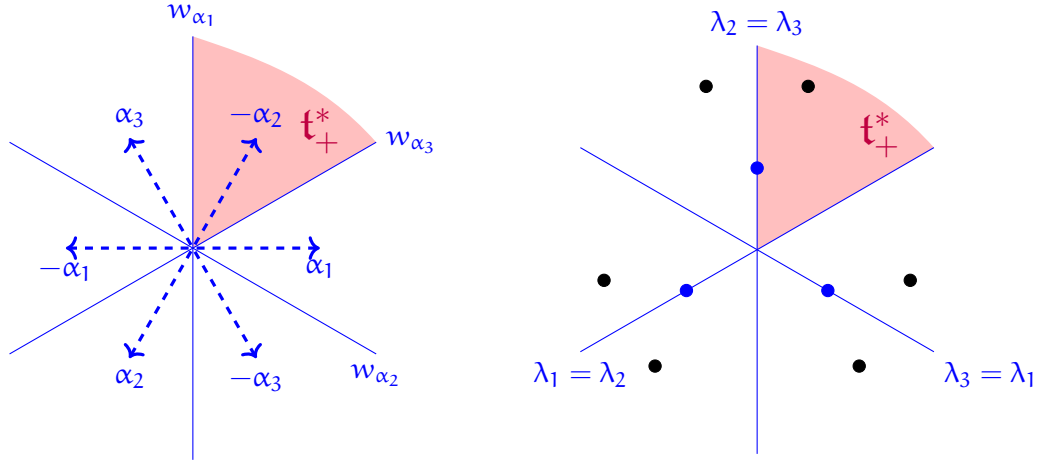


Figure 2.1: On the left the roots for $SU(3)$ and the area shaded in pink is the positive Weyl chamber \mathfrak{t}_+^* . The $\pm\alpha_i$ are the roots. On the right are shown two orbits of the Weyl group, the black dots show a generic orbit, the blue ones a degenerate orbit.

Conventions For future computations, especially in Section 4, we use the following notation and choices. For a basis of the Cartan subalgebra of $SU(3)$ consisting of diagonal matrices we take,

$$\xi_1 = \text{diag}[0, i, -i], \quad \xi_2 = \text{diag}[-i, 0, i]. \quad (2.5)$$

Here and in what follows, $\text{diag}[a, b, c]$ refers to the matrix with diagonal entries a, b, c and 0s elsewhere. The positive roots in $\mathfrak{su}(3)^*$ are chosen to be $\alpha_1, -\alpha_2$ and α_3 , where

$$\alpha_1 = \text{diag}[0, 1, -1], \quad \alpha_2 = \text{diag}[-1, 0, 1], \quad \alpha_3 = \text{diag}[1, -1, 0] \quad (2.6)$$

(letting α_2 be a negative root renders some later expressions more symmetric). See Figure 2.1. Notice that we represent elements of $\mathfrak{su}(3)$ as skew-hermitian matrices, but elements of the dual $\mathfrak{su}(3)^*$ as Hermitian matrices. This requires the pairing to be written as

$$\mu(\xi) \equiv \langle \mu, \xi \rangle = \text{Im}(\text{tr}(\mu\xi)), \quad (2.7)$$

for $\mu \in \mathfrak{su}(3)^*$ and $\xi \in \mathfrak{su}(3)$. Using this, one finds,

$$\begin{aligned} \alpha_1(\xi_1) &= 2, & \alpha_2(\xi_1) &= -1, & \alpha_3(\xi_1) &= -1 \\ \alpha_1(\xi_2) &= -1, & \alpha_2(\xi_2) &= 2, & \alpha_3(\xi_2) &= -1. \end{aligned} \quad (2.8)$$

With these conventions, the root space decomposition is

$$\mathfrak{g} = \mathfrak{t} \oplus \mathfrak{g}_{\alpha_1} \oplus \mathfrak{g}_{\alpha_2} \oplus \mathfrak{g}_{\alpha_3}, \quad (2.9)$$

where \mathfrak{g}_{α_1} consists of matrices of the form

$$\xi = \begin{pmatrix} 0 & 0 & 0 \\ 0 & 0 & a \\ 0 & -\bar{a} & 0 \end{pmatrix},$$

for $a \in \mathbb{C}$, and \mathfrak{g}_{α_2} (with all entries except ξ_{13}, ξ_{31} vanishing) and \mathfrak{g}_{α_3} similarly.

Witt-Artin decomposition Consider a symplectic G -manifold (M, Ω) , with G -equivariant momentum map $J : M \rightarrow \mathfrak{g}^*$, and let $m \in M$, and $\mu = J(m)$. Then $H = G_m$ acts symplectically on the tangent space $T_m M$. We recall the Witt-Artin decomposition of $T_m M$, see [12] for details.

Let $T = \mathfrak{g} \cdot m$. It follows from (2.1) that $T^\omega = \ker(DJ_m)$. Consider the four spaces:

$$\begin{aligned} T_0 &= T \cap T^\omega = \mathfrak{g}_\mu \cdot m, & T_1 &= T/T_0 \simeq \mathfrak{g}/\mathfrak{g}_\mu, \\ N_1 &= T^\omega/T_0, & N_0 &= T_m M/(T + T^\omega). \end{aligned} \quad (2.10)$$

The spaces T_0 and T_1 give a decomposition of the tangent space T to the group orbit $G \cdot m$ at m while N_0 and N_1 decompose its (or a) normal space. N_1 is the *symplectic slice* at m .

By simple linear algebra, the group action and symplectic form define isomorphisms (of representations of G_m),

$$T_0 \simeq \mathfrak{g}_\mu/\mathfrak{g}_m, \quad T_1 \simeq \mathfrak{g}/\mathfrak{g}_\mu, \quad N_0 \simeq T_0^*,$$

and there is a G_m -equivariant identification

$$T_m M \simeq T_0 \oplus T_1 \oplus N_1 \oplus N_0. \quad (2.11)$$

In particular, we make a choice for N_0 (modulo T_1) by requiring $DJ_m(N_0) \subset \mathfrak{g}_\mu^*$, which is possible since $DJ_m(T + T^\omega) = DJ_m(T_1) = \mathfrak{g}_\mu^\circ$. With this choice of N_0 it follows that

$$DJ_m(N_0) = \mathfrak{g}_\mu^* \cap \mathfrak{g}_m^\circ. \quad (2.12)$$

since $\text{Im}(DJ_m) = \mathfrak{g}_m^\circ$.

If $v \in T_m M$ we write its decomposition with respect to this identification as $v = (w, x, y, z)$, or

$$v = w + x + y + z \in T_0 \oplus T_1 \oplus N_1 \oplus N_0. \quad (2.13)$$

Finally, N_1 and T_1 are symplectic while N_0 and T_0 are isotropic (and paired by the symplectic form). More specifically, given any basis of T_0 there is a basis of N_0 such that the matrix of ω at m has the form

$$[\omega] = \begin{bmatrix} 0 & 0 & 0 & -I \\ 0 & \omega_{T_1} & 0 & 0 \\ 0 & 0 & \omega_{N_1} & 0 \\ I & 0 & 0 & 0 \end{bmatrix}.$$

Here ω_{T_1} is the KKS symplectic form on the coadjoint orbit described above, and ω_{N_1} is the natural symplectic form on the symplectic slice. For details see [12].

MGS normal form For an action of a compact group G on a manifold M , let $m \in M$ and let S be a slice to the orbit (which can be identified with a neighbourhood of 0 in the normal space N to the orbit). Then there is a tubular neighbourhood U of $G \cdot m$ which is equivariantly diffeomorphic to $U \simeq G \times_H S$, where $H = G_m$.

In the symplectic/Hamiltonian setting, this is refined by the Marle-Guillemin-Sternberg normal form, defined as follows, see for example [12, 15] and references therein for details. The

ingredients for this local model are, $\mu \in \mathfrak{t}_+^*$, a closed subgroup H of the stabilizer G_μ and a symplectic representation V of H . From this one forms a symplectic manifold

$$Y = Y(\mu, H, V) = G \times_H (\mathfrak{n} \oplus V),$$

where $\mathfrak{n} = \mathfrak{g}_\mu / \mathfrak{h}$. The momentum map is given by

$$J([g, \sigma, v]) = g(\mu + \sigma + J_V(v))g^{-1}, \quad (2.14)$$

where J_V is the homogeneous quadratic momentum map for the representation V ,

$$\langle J_V(v), \xi \rangle = \frac{1}{2} \omega_V(\xi v, v).$$

The momentum polytope for $Y(\mu, H, V)$ is

$$\Delta(\mu, H, V) = J(Y) \cap \mathfrak{t}_+^*.$$

Marle and independently Guillemin and Sternberg prove that, given $m \in M$, there is a G -invariant neighbourhood U of m and a G -invariant neighbourhood U' of $G \times_H (0 \times 0)$ in $Y(J(m), G_m, N_1)$ such that U and U' are equivalent as Hamiltonian G -spaces. Consequently, following Sjamaar [15] one makes the following definition:

Definition 2.1 Let $m \in M$ and let $\mu = J(m)$. The **local momentum cone** Δ_m is defined to be

$$\Delta_m := \Delta(\mu, G_m, N_1)$$

where N_1 is the symplectic slice at m . Denote also by δ_m the germ at μ of the set Δ_m ; we call δ_m the **infinitesimal momentum cone** at m .

Sjamaar proceeds to prove the following theorem.

Theorem 2.2 (Sjamaar [15]) Let M be a compact symplectic manifold with a Hamiltonian action of a compact Lie group G , and momentum map $J : M \rightarrow \mathfrak{g}^*$.

(1). If $J(m_1) = J(m_2)$ then $\Delta_{m_1} = \Delta_{m_2}$, and a fortiori the infinitesimal momentum cones δ_{m_1} and δ_{m_2} coincide.

(2). The momentum polytope of M is the intersection of all the local momentum cones:

$$\Delta(M) = \bigcap_{m \in \Phi^{-1}(\mathfrak{t}_+^*)} \Delta_m.$$

Moreover, for each m , the infinitesimal momentum cone δ_m coincides with the germ at μ of $\Delta(M)$.

(3). If the point μ is a vertex of the momentum polytope, then, for any $m \in J^{-1}(\mu)$,

$$\mathfrak{g}_m^\circ \cap \mathfrak{z}_\mu^* = 0.$$

Part (3) is stated in a different form by Sjamaar; this equivalent form is proved in [9]. In particular, from (3) it follows that a point in the interior of the positive Weyl chamber is a vertex then $G_m = \mathbb{T}$.

The statements regarding the infinitesimal momentum cones are not made by Sjamaar, though they are straightforward: by the Marle-Guillemin-Sternberg normal form theorem, there is an invariant neighbourhood of m whose image under the momentum map coincides with a neighbourhood of μ in Δ_m . Since the momentum map is locally G -open onto its image [11], it follows that any sufficiently small representative of the germ δ_m is a neighbourhood of μ in $\Delta(M)$.

From (1) we can replace Δ_m by Δ_μ for $\mu = J(m)$. It is not always straightforward to find the local momentum cone, although there are 2 cases where it is clear:

- Firstly, if $m \in J^{-1}(\mu)$ satisfies $\mathfrak{g}_m = 0$ then DJ_m is surjective, and $\Delta_\mu = \mathfrak{t}_+^*$.
- Secondly, if μ lies in the interior of the positive Weyl chamber, then $G_\mu = \mathbb{T}$ and G_m is a sub-torus. Then $DJ_m(N_0) = \mathfrak{g}_m^\circ \cap \mathfrak{t}^*$, and moreover, since G_m is a torus, the symplectic representation N_1 is a sum of 2-dimensional (symplectic) representations of G_m with weights $\beta_1, \dots, \beta_r \in \mathfrak{g}_m^* \subset \mathfrak{t}^*$ say. Then (see (2.2))

$$J_{N_1}(v_1, \dots, v_r) = \frac{1}{2} \sum_j \Gamma_j |v_j|^2 \beta_j \in \mathfrak{g}_m^*,$$

where the coefficients Γ_j depend on the symplectic form, and it follows that Δ_μ is the translation to μ of the Cartesian product of $\mathfrak{g}_m^\circ \cap \mathfrak{t}^*$ and $\text{Im}(J_{N_1}) \subset \mathfrak{g}_m^*$ inside \mathfrak{t}_+^* .

2.2 Momentum map for the $SU(3)$ action on products of \mathbb{CP}^2

We turn our attention to the example of interest, namely $G = SU(3)$ acting on \mathbb{CP}^2 . Now \mathbb{CP}^2 has a particular $SU(3)$ -invariant symplectic form known as the Fubini-Study form (obtained from the unit sphere $S^5 \subset \mathbb{C}^3$ by reduction by $U(1)$) and denoted ω_{FS} . All other invariant 2-forms on \mathbb{CP}^2 are scalar multiples of this basic one. The momentum map for the Fubini-Study form on \mathbb{CP}^2 is

$$\begin{aligned} J_0 : \mathbb{CP}^2 &\longrightarrow \mathfrak{su}(3)^* \\ Z &\longmapsto Z \otimes \bar{Z} - \frac{1}{3} I_3. \end{aligned} \tag{2.15}$$

Here $Z = [z_1 : z_2 : z_3] \in \mathbb{CP}^2$. Since we are viewing \mathbb{CP}^2 as the reduction of S^5 , it follows that $\sum |z_j|^2 = 1$, and the term $Z \otimes \bar{Z}$ is the Hermitian matrix $(z_i \bar{z}_j)$, whose trace is 1 whence the subtraction of the constant term involving the 3×3 identity matrix I_3 . Note that $Z \otimes \bar{Z}$ is a *Hermitian* matrix, while the elements of $\mathfrak{su}(3)$ are skew-Hermitian matrices. This is not a problem, as the sets of Hermitian and skew-Hermitian matrices are related simply by multiplication by i , and we define the pairing of $\mathfrak{su}(3)^*$ with $\mathfrak{su}(3)$ by the expression in (2.7). It is clear that the expression J_0 is equivariant, in that for $g \in SU(3)$,

$$J_0(gZ) = g J_0(Z) g^{-1}. \tag{2.16}$$

In particular, the image of J_0 consists of all 3×3 Hermitian matrices with eigenvalues $\frac{2}{3}, -\frac{1}{3}, -\frac{1}{3}$.

The phase space M we are interested in is the Cartesian product of N copies of \mathbb{CP}^2 , where the j^{th} copy of \mathbb{CP}^2 is endowed with an invariant symplectic form $\Gamma_j \omega_{\text{FS}}$. More formally, with $\pi_j : M \rightarrow \mathbb{CP}^2$ given by $\pi_j(Z_1, \dots, Z_N) = Z_j$, then the symplectic form on M is

$$\Omega := \sum_j \Gamma_j \pi_j^* \omega_{\text{FS}}.$$

We refer to this as the *weighted symplectic form* on M , with weights $\Gamma_1, \dots, \Gamma_N$. The momentum map $J : M \rightarrow \mathfrak{su}(3)^*$ for the $\text{SU}(3)$ -action on (M, Ω) is then given by

$$J : (Z_1, \dots, Z_N) \rightarrow \sum_{j=1}^N \Gamma_j J_0(Z_j), \quad Z_j \in \mathbb{CP}^2. \quad (2.17)$$

It is clear from (2.16) that this map is also equivariant for the diagonal action on M .

Since it is equivariant, J descends to a map between orbit spaces we call the *orbit momentum map* and denote \mathcal{J} , according to the following diagram,

$$\begin{array}{ccc} M & \xrightarrow{J} & \mathfrak{su}(3)^* \\ \downarrow & & \downarrow \\ M/G & \xrightarrow{\mathcal{J}} & \mathfrak{g}^*/G \end{array} \quad (2.18)$$

where the vertical maps are the quotient maps. Since every coadjoint orbit in \mathfrak{g}^* intersects \mathfrak{t}^* in a Weyl group orbit, one can identify \mathfrak{g}^*/G with a positive Weyl chamber \mathfrak{t}_+^* . By the Atiyah-Guillemin-Sternberg-Kirwan convexity theorem, the image $J(M)/G = \mathcal{J}(M/G)$ is a convex polytope in \mathfrak{t}_+^* , called the *momentum polytope*. For a given number of copies of \mathbb{CP}^2 , the shape of this polytope will depend on the weights Γ_j .

Remark 2.3 While we can identify \mathfrak{g}^*/G with \mathfrak{t}_+^* as described, one needs to be aware that this identification is a homeomorphism but not a diffeomorphism. Indeed there are many (eg linear) functions on \mathfrak{t}_+^* which are not the restriction of a smooth invariant function on \mathfrak{g}^* (nor Weyl group invariant on \mathfrak{t}^*). See Remark 2.5 below for further details on this point.

Remark 2.4 There is an important involution defined on \mathfrak{t}_+^* , denoted $*$, defined by

$$*\mu = w(-\mu)$$

where w is the (usually unique) element of the Weyl group that brings $-\mu$ back into the positive Weyl chamber. In the case of $\text{SU}(3)$ and the positive Weyl chamber shown in Figure 2.1, we have $w = w_2$. Thus $*\mu = -w_2\mu$; in Figure 2.2 this is the reflection in the line $\lambda_2 = 0$. The importance in our context is that if one changes $\Gamma = (\Gamma_1, \Gamma_2, \Gamma_3)$ to $-\Gamma$, then

$$\Delta_\Gamma(M) = *\Delta_{-\Gamma}(M).$$

For this reason it is sufficient to consider $\sum \Gamma_j \geq 0$.

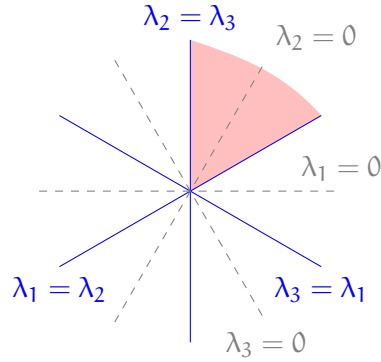


Figure 2.2: This shows the plane parametrized by three real numbers $\lambda_1, \lambda_2, \lambda_3$ which sum to zero. The orientation is such that λ_1 increases to the top of the diagram. Transpositions of the three numbers correspond to reflections in the blue lines. The pink region is where $\lambda_1 \geq \lambda_2 \geq \lambda_3$. These numbers will be the eigenvalues of a trace zero Hermitian matrix. (Cf. the roots shown in Figure 2.1)

2.3 Coadjoint orbits

We have chosen to represent elements of $\mathfrak{su}(3)^*$ as 3×3 Hermitian matrices of trace zero. The coadjoint action is by conjugation:

$$g \cdot A = gAg^\dagger$$

where $g^\dagger = g^{-1}$ is the conjugate transpose of $g \in \mathrm{SU}(3)$. As is well-known from linear algebra courses, two Hermitian matrices are conjugate if and only if they have the same spectrum (including multiplicities). Write this spectrum as $\sigma(A) = \{\lambda_1, \lambda_2, \lambda_3\}$, allowing for multiplicities in the set (sometimes called a multiset).

It follows that each coadjoint orbit corresponds to a triple of real numbers summing to zero, and this can be ordered so that $\lambda_1 \geq \lambda_2 \geq \lambda_3$; see Figure 2.2. Since the λ_j sum to 0, and each is non-zero, it follows that in the preferred ordering, $\lambda_1 > 0$ and $\lambda_3 < 0$, while the sign of λ_2 is variable. In the figure, the coordinate λ_2 increases as the point moves up or to the left.

Remark 2.5 Continuing Remark 2.3 above, we note here that the quotient map

$$\mathfrak{su}(3)^* \longrightarrow \mathfrak{su}(3)^*/\mathrm{SU}(3)$$

can be written as the map $A \mapsto (\chi_2(A), \chi_3(A))$ — the coefficients of the characteristic polynomial of A , which is a smooth and G -invariant map. However the map

$$\mathfrak{su}(3)^* \longrightarrow \mathfrak{t}_+^*$$

which maps A to its three eigenvalues, is not smooth but involves extracting roots of the characteristic polynomial.

2.4 Action of $SU(3)$ on products of \mathbb{CP}^2

Let $Z = [z_1 : z_2 : z_3] \in \mathbb{CP}^2$, then $A \in SU(3)$ acts in a natural way on this point: if $Z' = AZ$ then $z'_j = \sum_k A_{jk} z_k$. Given any $Z \in \mathbb{CP}^2$, the stabilizer $G_Z \simeq U(2)$ is as follows. Consider for example $Z = [1 : 0 : 0]$, then $AZ = Z$ if and only if A has the block form

$$A = \begin{pmatrix} (\det A_1)^{-1} & 0 \\ 0 & A_1 \end{pmatrix} \quad (2.19)$$

where $A_1 \in U(2)$. Since $SU(3)$ acts transitively on \mathbb{CP}^2 the stabilizer of any other point will be conjugate to this particular $U(2)$ subgroup. In terms of the root decomposition (2.9) of the Lie algebra, this particular copy of $U(2)$ has $\mathfrak{u}(2) = \mathfrak{t} \oplus \mathfrak{g}_{\alpha_1}$. (The stabilizer of e_j has Lie algebra equal to $\mathfrak{t} \oplus \mathfrak{g}_{\alpha_j}$.)

Now consider the diagonal action on $M = \mathbb{CP}^2 \times \mathbb{CP}^2$, and let $m = (Z_1, Z_2) \in M$. Let us suppose that $Z_1 = e_1 = [1 : 0 : 0]$. For Z_2 there are 3 cases to consider: first if $Z_1 = Z_2$ (that is, m is a point on the diagonal) then G_m is again $U(2)$. Next, if Z_2 and Z_1 are perpendicular, then we may take $Z_2 = e_2 = [0 : 1 : 0]$ and the stabilizer is the (maximal) torus \mathbb{T}^2 consisting of diagonal matrices:

$$\mathbb{T}^2 = \left\{ \text{diag}[e^{i\theta}, e^{i\phi}, e^{i\psi}] \mid \theta + \phi + \psi = 0 \pmod{2\pi} \right\}.$$

Finally, if Z_1, Z_2 are in general position (neither equal nor perpendicular) then the stabilizer is just a copy of $U(1)$. For example if $Z_2 = [1 : 1 : 0]$ then the stabilizer of $(e_1, Z_2) \in M$ is the subgroup of \mathbb{T}^2 consisting of matrices of the form

$$\left\{ \text{diag}[e^{i\theta}, e^{i\theta}, e^{-2i\theta}] \right\} \simeq U(1).$$

We summarize these possibilities in the following table,

geometry of m	stabilizer
on diagonal	$U(2)$
(u, u^\perp)	\mathbb{T}^2
general position	$U(1)$

(2.20)

where u and u^\perp are any pair of orthogonal points in \mathbb{CP}^2 .

For a product of three copies of \mathbb{CP}^2 the analysis is similar. We have:

geometry	stabilizer
on diagonal	$U(2)$
(u, u, v)	\mathbb{T}^2
(u, v, w)	\mathbb{T}^2
(u, u', v)	$U(1)$
spanning a plane	$U(1)$
general position	$\mathbf{1}$

(2.21)

Here u, v and w are pairwise orthogonal, while u, u' are distinct but not orthogonal, and v is orthogonal to both u and u' .

The following lemma will be useful when computing local momentum cones in Section 4. Recall that $e_1 = [1 : 0 : 0] \in \mathbb{CP}^2$ etc.. Recall also that given a complex representation V of \mathbb{T} , the form $\alpha \in \mathfrak{t}^*$ is a weight if the weight-space V_α is non-zero, where

$$V_\alpha = \{v \in V \mid \xi v = i\alpha(\xi)v, \forall \xi \in \mathfrak{t}\}.$$

Lemma 2.6 *The representation of \mathbb{T}^2 on the tangent space $T_{e_i}\mathbb{CP}^2$, has the following weights:*

$$T_{e_1}\mathbb{CP}^2 = -\alpha_3 \oplus \alpha_2, \quad T_{e_2}\mathbb{CP}^2 = -\alpha_1 \oplus \alpha_3, \quad T_{e_3}\mathbb{CP}^2 = -\alpha_2 \oplus \alpha_1.$$

See (2.6) for the definition of the α_j ; the choice of \pm -signs in each case is determined by the natural complex structure on $T_{e_j}\mathbb{CP}^2$. This sign is compatible with the symplectic structure if the corresponding symplectic weight satisfies $\Gamma > 0$.

Proof. For $T_{e_1}\mathbb{CP}^2$, the tangent vectors are of the form $\mathbf{x} = (0, v, w)^T$ (with $v, w \in \mathbb{C}$), and the action of ξ_1 on this is $\xi_1.(0, v, w)^T = (0, iv, -iw)^T$, and $\xi_2.(0, v, w)^T = (0, iv, 2iw)^T$. Note that the action of ξ_2 has to be adjusted to ensure it fixes e_1 ; the matrix $\text{diag}[0, i, 2i]$ acts the same as the one given in (2.5), and this one manifestly fixes e_1 and hence acts on $T_{e_1}\mathbb{CP}^2$ by simple multiplication. Thus, $(0, v, 0)^T$ has weight satisfying $\alpha(\xi_1) = \alpha(\xi_2) = 1$, hence its weight is $-\alpha_3$, while $(0, 0, w)^T$ has weight satisfying $\alpha(\xi_1) = -1$ and $\alpha(\xi_2) = 2$, giving the weight α_2 . The other cases are similar. In particular, $\mathbf{x} \in T_{e_2}\mathbb{CP}^2$ can be written $\mathbf{x} = (u, 0, w)^T \in \mathbb{C}^2$ and the weight of $(0, 0, w)^T$ is $-\alpha_1$ while that of $(u, 0, 0)^T$ is α_3 . Finally, $\mathbf{x} \in T_{e_3}\mathbb{CP}^2$ can be written $\mathbf{x} = (u, v, 0)^T \in \mathbb{C}^2$ and the weight of $(u, 0, 0)^T$ is $-\alpha_2$ while that of $(0, v, 0)^T$ is α_1 . \square

3 Momentum polytopes for $\text{SU}(3)$ action on $\mathbb{CP}^2 \times \mathbb{CP}^2$

To determine these polytopes one can apply a far simpler argument than for the product of 3 copies, as we shall see. This example has been considered before by Bedulli and Gori [2].

The action of $\text{SU}(3)$ on $M = \mathbb{CP}^2 \times \mathbb{CP}^2$ is not transitive, and it is not hard to see that (Z_1, Z_2) and (Z'_1, Z'_2) lie in the same orbit if and only if the distance between Z_1 and Z_2 is equal to that between Z'_1 and Z'_2 . It follows that the orbit space $M/\text{SU}(3)$ is a compact line segment, parametrized by this distance. The image of the orbit momentum map \mathcal{J} is therefore 1-dimensional, and by the convexity theorem it must be a line segment (or a point). A line segment has two ends, and it suffices to find these two end points, which will necessarily be the images of the end-points of $M/\text{SU}(3)$.

Theorem 3.1 *The momentum polytopes $\Delta(M)$ of the $\text{SU}(3)$ action on $M = \mathbb{CP}^2 \times \mathbb{CP}^2$ with weighted symplectic form $\Gamma_1\omega_{\text{FS}} \oplus \Gamma_2\omega_{\text{FS}}$ with $\Gamma_i \neq 0$ fall into four different types for which $\Gamma_1 \neq \pm\Gamma_2$, and three transitional ones where $\Gamma_1 = \pm\Gamma_2$; these are shown in Figures 3.1 and 3.2 respectively.*

Remark 3.2 We have not defined what we mean by the *type* of a momentum polytope. Without giving a formal definition, the type is a combination of ‘combinatorics’ and ‘geometry’ within the positive Weyl chamber. For example in Figure 3.1, (a) and (b) have the same ‘combinatorics’ (indeed all 4 figures do), but their geometry relative to the Weyl chamber is different.

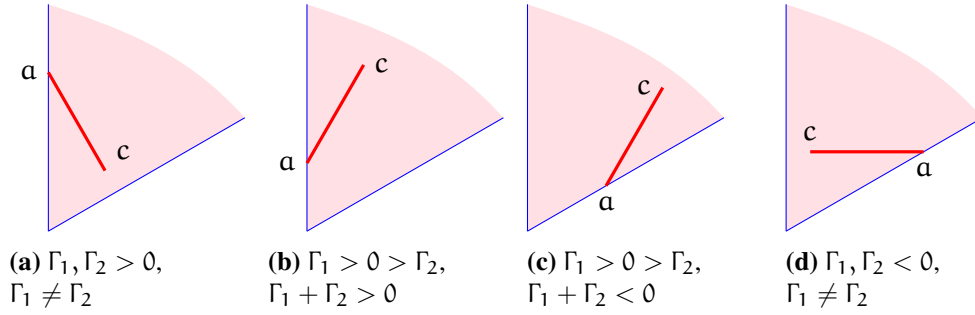


Figure 3.1: The four generic polytopes for the action of $SU(3)$ on $\mathbb{CP}^2 \times \mathbb{CP}^2$. In each case a represents the image of points of the form (u, u) , and c of points of the form (u, u^\perp) . Notice that all these polytope-segments are parallel to one of the roots (equivalently, orthogonal to one of the walls of the Weyl chamber). Notice that figures (a) and (d) are related by the involution $*$ of Remark 2.4, as are figures (b) and (c).

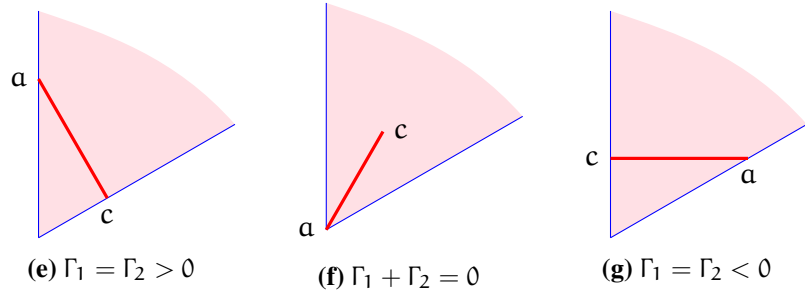


Figure 3.2: The three transitional polytopes for the action of $SU(3)$ on $\mathbb{CP}^2 \times \mathbb{CP}^2$. See the caption of Figure 3.1 for explanations of notation, and Remark 3.3 for discussion. Note that the involution $*$ exchanges figures (e) and (g) and leaves (f) unchanged.

Proof. First let us find the images of the momentum map for the points in M at extrema of the distance. It suffices to choose representatives: for minimal distance we have $m = (e_1, e_1)$ with $e_1 = [1 : 0 : 0]$ and for maximal distance we chose points that are perpendicular, for example (e_1, e_2) , with $e_2 = [0 : 1 : 0]$. From (2.15) and (2.17) one finds,

$$J(e_1, e_2) = \frac{1}{3}\Gamma_1 \begin{pmatrix} 2 & 0 & 0 \\ 0 & -1 & 0 \\ 0 & 0 & -1 \end{pmatrix} + \frac{1}{3}\Gamma_2 \begin{pmatrix} -1 & 0 & 0 \\ 0 & 2 & 0 \\ 0 & 0 & -1 \end{pmatrix}.$$

From this and a similar calculation for $J(e_1, e_1)$ we obtain the spectra,

$$\begin{aligned} \sigma(J(e_1, e_1)) &= \left\{ \frac{2(\Gamma_1 + \Gamma_2)}{3}, \frac{-(\Gamma_1 + \Gamma_2)}{3}, \frac{-(\Gamma_1 + \Gamma_2)}{3} \right\}, \\ \sigma(J(e_1, e_2)) &= \left\{ \frac{(2\Gamma_1 - \Gamma_2)}{3}, \frac{(2\Gamma_2 - \Gamma_1)}{3}, \frac{-(\Gamma_1 + \Gamma_2)}{3} \right\}. \end{aligned}$$

Notice that the first of these spectra has two equal eigenvalues so lies on a line of reflection.

When ordered by decreasing value, this point is marked α in each diagram. All three are equal if and only if $\Gamma_1 + \Gamma_2 = 0$, and in that case α lies at the origin. The other point $c = J(e_1, e_2)$ generically has 3 distinct elements, so does not lie on a line of reflection. Repeated eigenvalues occur if and only if $\Gamma_1 = \Gamma_2$, as is readily checked (or if one of the Γ_j vanishes, which we are excluding), and the corresponding point is marked c in the two figures.

There remains to show that the points α, c are indeed the endpoints of the segment $\Delta(M)$ as claimed. Clearly, since α lies on a wall of the Weyl chamber, it must be an endpoint of the segment. Now any endpoint is a vertex of the polytope so corresponds either to a point in the wall or a fixed point for the torus action, but α and c are the only images of fixed points. \square

Remark 3.3 As (Γ_1, Γ_2) varies in the plane there are transitions that occur at the points described in the theorem. Here we briefly describe these.

First, as $\Gamma_1 + \Gamma_2$ goes from being positive to negative, the transition from Figure 3.1b to 3.1c is seen clearly through Figure 3.2f. When $\Gamma_1 + \Gamma_2 = 0$ one of the eigenvalues vanishes for both points α and c so the segment lies along the line $\lambda_2 = 0$.

The transition between Figures 3.1a and 3.1b occur as Γ_2 changes sign. As $\Gamma_2 \rightarrow 0$, the segment in Figure 3.1a or 3.1b becomes shorter, and in the limit becomes just the point α (when the symplectic form is degenerate, the momentum map does not ‘see’ the second factor in the product M , and the momentum polytope reduces to that of \mathbb{CP}^2 which is just a single point). The transition between Figures 3.1c and 3.1d is similar.

Finally, the transitional figures shown in Figures 3.2e and 3.2g occur when $\Gamma_1 = \Gamma_2$ and $J(e_1, e_2)$ has a double eigenvalue. As say, Γ_1 decreases through the value Γ_2 from $\Gamma_1 > \Gamma_2 > 0$ to $\Gamma_2 > \Gamma_1 > 0$, the segment in Figure 3.1a extends until it hits the right-hand wall (as in Fig. 3.2e) and then retreats back to look like the segment in Figure 3.1a again.

Proof of Theorem 1.1 (Part 1). Consider $M = \mathbb{CP}^2 \times \mathbb{CP}^2$, with $\Gamma_1 = -3\lambda_A$ and $\Gamma_2 = -3\lambda_B$. The two extremes of the segment have spectra given above

$$\begin{aligned}\sigma(J(e_1, e_1)) &= \{\lambda_A + \lambda_B, \lambda_A + \lambda_B, -2(\lambda_A + \lambda_B)\}, \\ \sigma(J(e_1, e_2)) &= \{\lambda_A + \lambda_B, \lambda_A - 2\lambda_B, \lambda_B - 2\lambda_A\}.\end{aligned}$$

Then $\lambda_1 = \lambda_A + \lambda_B$, while λ_2 lies between $\lambda_A + \lambda_B$ and $\lambda_A - 2\lambda_B$ as stated in the theorem. \square

4 Momentum polytopes for $SU(3)$ action on $\mathbb{CP}^2 \times \mathbb{CP}^2 \times \mathbb{CP}^2$

Now let $M = \mathbb{CP}^2 \times \mathbb{CP}^2 \times \mathbb{CP}^2$. Recall from Section 2.2, the momentum map for the $SU(3)$ action on the manifold M is

$$J : (Z_1, Z_2, Z_3) \mapsto \sum_{j=1}^3 \Gamma_j Z_j \otimes \bar{Z}_j - \frac{1}{3} \left(\sum_{j=1}^3 \Gamma_j \right) I_3$$

with $Z_1, Z_2, Z_3 \in \mathbb{CP}^2$, see (2.15).

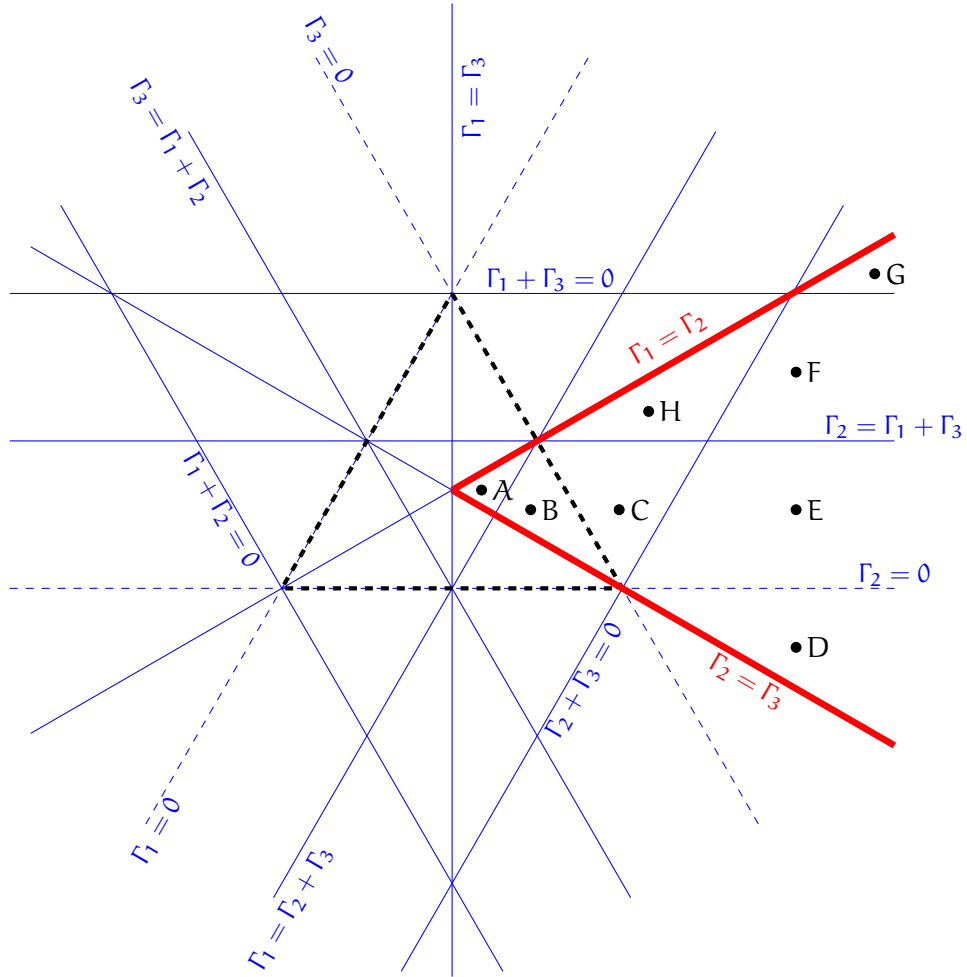


Figure 4.1: This shows the parameter plane $\Gamma_1 + \Gamma_2 + \Gamma_3 = \text{const}$ with $\text{const} > 0$. Within the central black triangle all 3 weights are positive. The value of Γ_2 is constant on horizontal lines and increases vertically upwards; variations of the other variables can be deduced from this. The blue lines indicate where the polytope type changes, see Table 4.1. The sector between the red lines is where $\Gamma_1 \geq \Gamma_2 \geq \Gamma_3$. The generic polytope types are labelled A, B, ..., H, and illustrated in Fig. 4.2, and the respective transitions are labelled AB, CE etc., see Fig. 4.5.

Theorem 4.1 *The momentum polytopes of the $SU(3)$ action on $\mathbb{CP}^2 \times \mathbb{CP}^2 \times \mathbb{CP}^2$ with weighted symplectic form $\Omega = \Gamma_1 \omega_{FS} \oplus \Gamma_2 \omega_{FS} \oplus \Gamma_3 \omega_{FS}$ (with $\Gamma_j \neq 0$) fall into eight different types for which $\Gamma_i - \Gamma_j - \Gamma_k \neq 0$, $\Gamma_i \pm \Gamma_j \neq 0$, where $i, j, k = 1, 2, 3$, and $\Gamma_1 + \Gamma_2 + \Gamma_3 > 0$. An example of each type is shown in Figure 4.2, while the 8 different regions of Γ -space are illustrated in Figure 4.1.*

Remark 4.2 There are another 8 types of generic momentum polytope with $\Gamma_1 + \Gamma_2 + \Gamma_3 < 0$. Note from the expression for J above, if the signs of all three Γ_j are changed, then the sign of J changes. This implies that the original polytope and the new one are related by the involution $*$ described in Remark 2.4. The cases with $\Gamma_1 + \Gamma_2 + \Gamma_3 = 0$ are transitional and described with other transitional cases further below—see Figure 4.7.

The remainder of this section consists of a proof of this theorem. See Remark 3.2 for a discussion of the word ‘type’. Non-generic, or transitional, polytopes are discussed in Section 4.2, and illustrated in diagrams at the end of the paper.

Recall from Sjamaar’s theorem 2.2 that if a point μ in the interior of the positive Weyl chamber is a vertex of the momentum polytope then there is an $m \in M$ with $J(m) = \mu$ and stabilizer equal to a maximal torus. We begin therefore with an analysis of the points with stabilizer equal to a maximal torus, which we choose to be the subgroup \mathbb{T} of diagonal matrices.

The fixed points of \mathbb{T} are the 27 points $(e_i, e_j, e_k) \in M$, where each $e_\ell \in \{e_1, e_2, e_3\}$ and $e_1 = [1 : 0 : 0]$, $e_2 = [0 : 1 : 0]$ and $e_3 = [0 : 0 : 1]$. The images in t_+^* of these points are determined by the spectra σ of the corresponding Hermitian matrix. Extending the notation for $\mathbb{CP}^2 \times \mathbb{CP}^2$, let

$$\begin{aligned} a &= \sigma\left(J(e_1, e_1, e_1)\right), & b &= \sigma\left(J(e_1, e_2, e_3)\right), \\ c_1 &= \sigma\left(J(e_2, e_1, e_1)\right), & c_2 &= \sigma\left(J(e_1, e_2, e_1)\right), & c_3 &= \sigma\left(J(e_1, e_1, e_2)\right). \end{aligned}$$

Here some caution is required: for example (e_1, e_1, e_1) and (e_2, e_2, e_2) and (e_3, e_3, e_3) lie on the same $SU(3)$ -orbit in M , and hence their values under J lie on the same Weyl group orbit in t^* . Only one of these will lie in the positive Weyl chamber (we denote this value a). On the other hand, their (unordered) spectra coincide, and so we consider spectra as sets. The same applies to say (e_1, e_2, e_1) —permuting the indices to, for example, (e_2, e_3, e_2) will give points in the same orbit (but not the same orbit as (e_2, e_1, e_1)), so their unordered spectra are equal (but in general different to that of (e_2, e_1, e_1)).

One finds

$$\begin{aligned} a &= \left\{ \frac{2}{3} (\Gamma_1 + \Gamma_2 + \Gamma_3), -\frac{1}{3} (\Gamma_1 + \Gamma_2 + \Gamma_3), -\frac{1}{3} (\Gamma_1 + \Gamma_2 + \Gamma_3) \right\}, \\ b &= \left\{ \frac{1}{3} (2\Gamma_1 - \Gamma_2 - \Gamma_3), \frac{1}{3} (-\Gamma_1 + 2\Gamma_2 - \Gamma_3), \frac{1}{3} (-\Gamma_1 - \Gamma_2 + 2\Gamma_3) \right\}, \\ c_1 &= \left\{ \frac{1}{3} (2\Gamma_1 - \Gamma_2 - \Gamma_3), \frac{1}{3} (-\Gamma_1 + 2\Gamma_2 + 2\Gamma_3), -\frac{1}{3} (\Gamma_1 + \Gamma_2 + \Gamma_3) \right\}, \\ c_2 &= \left\{ \frac{1}{3} (-\Gamma_1 + 2\Gamma_2 - \Gamma_3), \frac{1}{3} (2\Gamma_1 - \Gamma_2 + 2\Gamma_3), -\frac{1}{3} (\Gamma_1 + \Gamma_2 + \Gamma_3) \right\}, \\ c_3 &= \left\{ \frac{1}{3} (-\Gamma_1 - \Gamma_2 + 2\Gamma_3), \frac{1}{3} (2\Gamma_1 + 2\Gamma_2 - \Gamma_3), -\frac{1}{3} (\Gamma_1 + \Gamma_2 + \Gamma_3) \right\}. \end{aligned} \tag{4.1}$$

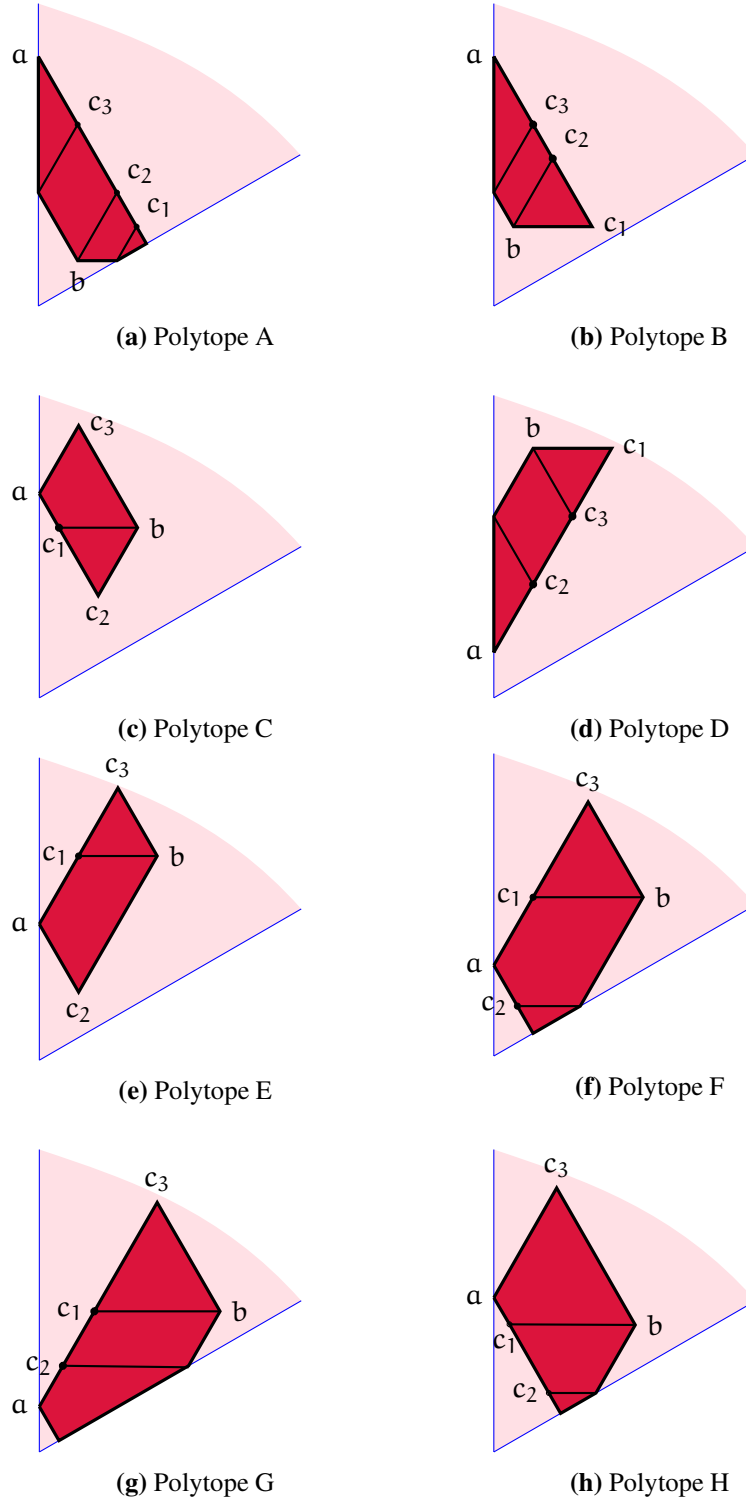


Figure 4.2: The generic momentum polytopes: refer to Fig. 4.1 for the notation.

condition	degeneracy
$\Gamma_1 = 0$	$a = c_1, b = c_2 = c_3$
$\Gamma_1 = \Gamma_2$	$b \in \text{Wall}, c_2 = c_3$
$\Gamma_1 + \Gamma_2 = 0$	$a = c_3 (\in \text{Wall})$
$\Gamma_1 = \Gamma_2 + \Gamma_3$	$c_1 \in \text{Wall}$
$\Gamma_1 + \Gamma_2 + \Gamma_3 = 0$	$a = 0$

Table 4.1: Transition values of Γ_j ; similar transitions occur permuting the indices. ‘ $x \in \text{Wall}$ ’ means that the point x belongs to a wall of the Weyl chamber. See Figure 4.1; further details are shown in Section 4.2 and Figures 4.5–4.9.

In order to depict them in the positive Weyl chamber, each of these sets should be ordered by $\lambda_1 \geq \lambda_2 \geq \lambda_3$. Note that point a always lies on a wall of the Weyl chamber as two of the eigenvalues are equal. The other points do not lie on a wall in general (when the 3 eigenvalues are distinct), however for some values of the weights the points can lie on the wall and these determine the transition cases.

For example, b lies on a wall if two of the weights coincide, while c_1 lies on a wall if $\Gamma_1 = \Gamma_2 + \Gamma_3$ or $\Gamma_2 + \Gamma_3 = 0$ (or the degenerate case $\Gamma_1 = 0$ which we exclude from disussions). Similar possibilities occur for c_2 and c_3 with the indices of the Γ_j permuted accordingly. The set of possible degeneracies, up to permutations of the indices, are listed in Table 4.1.

For some values of the symplectic weights Γ_j , the convex hull of these 5 points is equal to the momentum polytope. But for others we need to determine the ‘local momentum cones’, which are determined by the local images of the orbit momentum map near these points.

There are two procedures that can be used for drawing the different momentum polytopes. One is starting with one we know (eg for 2 copies of \mathbb{CP}^2 by putting one of the γ_j to 0) and then varying the weights and following the possible polytope, and the other is looking at the local momentum cones for each vertex. In this paper we use mostly the local momentum cones, with some continuity arguments, while in the thesis [14] the former approach is used more.

4.1 Generic polytopes

We now proceed to calculate the local momentum cones at each of the 5 vertices a, b, c_1, c_2 and c_3 . To do this we need to calculate J_{N_1} for each. At each of the \mathbb{T} -fixed points $m = (e_i, e_j, e_k)$ the tangent space at m is given by

$$T_m M = T_{e_i} \mathbb{CP}^2 \times T_{e_j} \mathbb{CP}^2 \times T_{e_k} \mathbb{CP}^2,$$

and this (symplectic) decomposition is invariant under the action of the maximal torus \mathbb{T} ; see Lemma 2.6 for the weights of this action.

Vertex b Consider the weights at $b = J(m)$ for $m = (e_1, e_2, e_3)$. If we put,

$$x = \left(\begin{pmatrix} 0 \\ v_1 \\ w_1 \end{pmatrix}, \begin{pmatrix} u_2 \\ 0 \\ w_2 \end{pmatrix}, \begin{pmatrix} u_3 \\ v_3 \\ 0 \end{pmatrix} \right) \in T_m M,$$

then,

$$DJ_m(\mathbf{x}) = \Gamma_1 \begin{pmatrix} 0 & \bar{v}_1 & \bar{w}_1 \\ v_1 & 0 & 0 \\ w_1 & 0 & 0 \end{pmatrix} + \Gamma_2 \begin{pmatrix} 0 & u_2 & 0 \\ \bar{u}_2 & 0 & \bar{w}_2 \\ 0 & w_2 & 0 \end{pmatrix} + \Gamma_3 \begin{pmatrix} 0 & 0 & u_3 \\ 0 & 0 & v_3 \\ \bar{u}_3 & \bar{v}_3 & 0 \end{pmatrix}$$

Thus $\ker DJ_m$ consists of those \mathbf{x} satisfying

$$\Gamma_1 \bar{v}_1 + \Gamma_2 u_2 = 0, \quad \Gamma_2 \bar{w}_2 + \Gamma_3 v_3 = 0, \quad \Gamma_1 w_1 + \Gamma_3 \bar{u}_3 = 0.$$

This defines a subspace of dimension 6. For this section, we assume \mathbf{b} is not contained in a wall of the Weyl chamber, and then this is in fact the symplectic slice: whenever $G_m = G_\mu$ one has $T_0 = 0 = N_0$, and thus $N_1 = \ker DJ_m$.

To find J_{N_1} is simple: since N_1 is the sum of 3 distinct representations, with weights α_1, α_2 and α_3 respectively, the momentum map is a sum of three terms (see (2.2)). Thus, using w_1, u_2, v_3 to parametrize N_1 (with $v_1 = -(\Gamma_2/\Gamma_1)\bar{u}_2$ etc.)

$$J_{N_1}(w_1, u_2, v_3) = \frac{\Gamma_3}{\Gamma_2}(\Gamma_2 - \Gamma_3)|v_3|^2 \alpha_1 + \frac{\Gamma_1}{\Gamma_3}(\Gamma_3 - \Gamma_1)|w_1|^2 \alpha_2 + \frac{\Gamma_2}{\Gamma_1}(\Gamma_1 - \Gamma_2)|u_2|^2 \alpha_3. \quad (4.2)$$

This determines the momentum cone at \mathbf{b} depending on the signs of the coefficients; it turns out that provided the three weights are distinct, this is always a 120° cone (if 2 of the weights coincide it becomes a 60° cone, but in that case \mathbf{b} is contained in a wall of the Weyl chamber—see further below for this case). For example, if $\Gamma_1 = 4, \Gamma_2 = 2, \Gamma_3 = -1$ (which lies in region C in Figure 4.1) then $\mathbf{b} = (7, 1, -8) \in \mathfrak{t}_+^*$ and

$$J_{N_1}(u_2, v_3, w_1) = -\frac{3}{2}|v_3|^2 \alpha_1 + 20|w_1|^2 \alpha_2 + |u_2|^2 \alpha_3,$$

whose image is precisely the cone at \mathbf{b} shown in Figure 4.2c (see Figure 2.1 for the definition of the α_j).

This expression is only the local momentum cone at \mathbf{b} provided $J(\mathbf{m}) \in \mathfrak{t}_+^*$; if that is not the case then the calculation needs repeating for whichever of the 6 equivalent points does map to \mathbf{b} . For example, if the weights Γ_j are such that $\mathbf{b} = J(\mathbf{m})$ for $\mathbf{m} = (e_2, e_1, e_3)$ then the expression for the local momentum cone (i.e., for J_{N_1}) is like the one above, but with the roots permuted by the appropriate element of the Weyl group; thus, in that case,

$$J_{N_1}(w_1, v_2, u_3) = \frac{\Gamma_1}{\Gamma_3}(\Gamma_1 - \Gamma_3)|w_1|^2 \alpha_1 + \frac{\Gamma_3}{\Gamma_2}(\Gamma_3 - \Gamma_2)|u_3|^2 \alpha_2 + \frac{\Gamma_2}{\Gamma_1}(\Gamma_2 - \Gamma_1)|v_2|^2 \alpha_3.$$

The choice we have made, that $\Gamma_1 \geq \Gamma_2 \geq \Gamma_3$, indeed ensures $J(e_1, e_2, e_3) \in \mathfrak{t}_+^*$.

Vertices c_j The calculations for c_1, c_2 and c_3 are very similar. For example, with $\mathbf{m} = (e_1, e_2, e_2)$ the elements of $T_m M$ can be written

$$\mathbf{x} = \left(\begin{pmatrix} 0 \\ v_1 \\ w_1 \end{pmatrix}, \begin{pmatrix} u_2 \\ 0 \\ w_2 \end{pmatrix}, \begin{pmatrix} u_3 \\ 0 \\ w_3 \end{pmatrix} \right) \in T_m M.$$

Then

$$\mathbf{x} \in \ker DJ_m \iff w_1 = (\Gamma_2 w_2 + \Gamma_3 w_3) = (\Gamma_1 \overline{v_1} + \Gamma_2 u_2 + \Gamma_3 u_3) = 0.$$

After similar calculations for other c_j , one obtains the following expressions for the slice momentum map.

- For c_1 using $m = (e_1, e_2, e_2)$,

$$J_{N_1} = -\frac{\Gamma_2}{\Gamma_3}(\Gamma_2 + \Gamma_3)|w_2|^2 \alpha_1 + \left(\frac{\Gamma_1}{\Gamma_2}(\Gamma_1 - \Gamma_2)|v_1|^2 + \frac{\Gamma_1 \Gamma_3}{\Gamma_2}(u_3 v_1 + \overline{u_3 v_1}) + \frac{\Gamma_3}{\Gamma_2}(\Gamma_3 + \Gamma_2)|u_3|^2 \right) \alpha_3. \quad (4.3)$$

Lemma 4.3 below shows that the coefficient of α_3 is definite if and only if

$$\Gamma_1 \Gamma_2 \Gamma_3 (\Gamma_1 - \Gamma_2 - \Gamma_3) > 0.$$

If this inequality is satisfied then c_1 lies at a vertex of the momentum polytope; if, on the other hand, it the expression is negative, then c_1 lies on an edge of the polytope (parallel to α_3). The given inequality is satisfied only in regions B and D.

- For c_2 using $m = (e_2, e_1, e_2)$, one obtains

$$J_{N_1} = -\frac{\Gamma_3}{\Gamma_1}(\Gamma_1 + \Gamma_3)|w_3|^2 \alpha_1 + \left(\frac{\Gamma_2}{\Gamma_3}(\Gamma_2 - \Gamma_3)|v_2|^2 + \frac{\Gamma_1 \Gamma_2}{\Gamma_3}(u_1 v_2 + \overline{u_1 v_2}) + \frac{\Gamma_1}{\Gamma_3}(\Gamma_1 + \Gamma_3)|u_1|^2 \right) \alpha_3. \quad (4.4)$$

- Finally, for c_3 using $m = (e_2, e_2, e_1)$,

$$J_{N_1} = -\frac{\Gamma_1}{\Gamma_2}(\Gamma_1 + \Gamma_2)|w_1|^2 \alpha_1 + \left(\frac{\Gamma_3}{\Gamma_1}(\Gamma_3 - \Gamma_1)|v_3|^2 + \frac{\Gamma_2 \Gamma_3}{\Gamma_1}(u_2 v_3 + \overline{u_2 v_3}) + \frac{\Gamma_2}{\Gamma_1}(\Gamma_1 + \Gamma_2)|u_2|^2 \right) \alpha_3. \quad (4.5)$$

Similar conditions on the Γ_j based on Lemma 4.3 ensure the coefficients of α_3 are definite or not.

As with b , if $J(m)$ fails to belong to the positive Weyl chamber, then the appropriate element of the Weyl group should be applied to the roots. It turns out that $J(e_1, e_2, e_2) \in \mathfrak{t}_+^*$ if and only if $\Gamma_1 + \Gamma_2 \geq \Gamma_3 \geq 0$. Notice that while J_{N_1} for b has all 3 roots appearing, for c_1, c_2 and c_3 it only has two distinct roots, which explains why only 2 lines (or half-lines) pass through those points in the figures.

Lemma 4.3 *The real quadratic form $q : \mathbb{C}^2 \rightarrow \mathbb{R}$ given by*

$$q(u, v) = A|u|^2 + B(u\overline{v} + \overline{u}v) + C|v|^2$$

is definite if and only if $AC > B^2$.

The proof is a simple calculation.

Vertex α : There remains to consider the point α . Let m be a point on the diagonal, and to be specific we take $m = (e_1, e_1, e_1)$. The stabilizer of m is now

$$G_m = \left\{ \begin{pmatrix} (\det A)^{-1} & 0 \\ 0 & A \end{pmatrix} \mid A \in U(2) \right\} \simeq U(2).$$

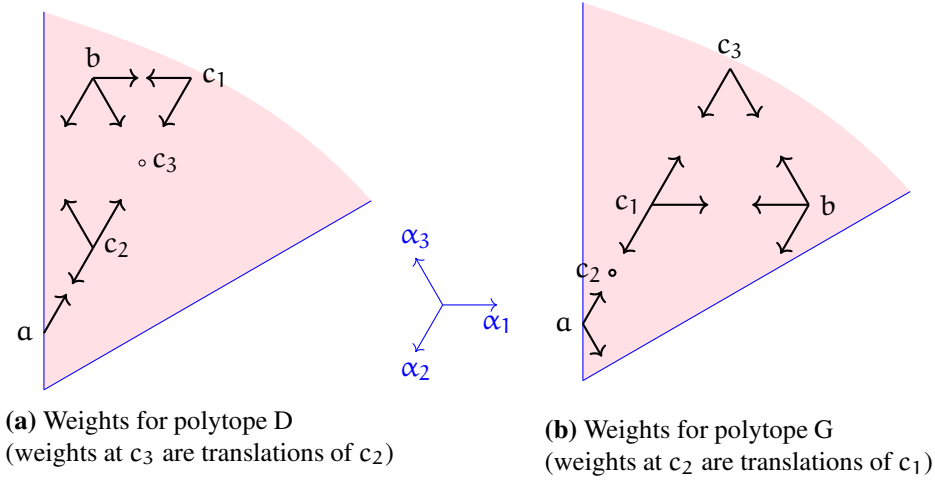


Figure 4.3: Examples showing weights at the fixed points

We assume $\sum_j \Gamma_j \neq 0$, in which case $\alpha = J(m) \neq 0$ (see (4.1)); the other case is covered by a continuity argument discussed below. We now have $J_{N_1} : N_1 \rightarrow \mathfrak{u}(2)^* \subset \mathfrak{su}(3)^*$.

Since again $G_\mu = G_m$, it follows that $T_0 = N_0 = 0$ and $N_1 = \ker DJ_m$, which is of dimension 8. Thus,

$$\mathbf{x} \in N_1 \iff \sum \Gamma_j v_j = \sum \Gamma_j w_j = 0.$$

Before solving for v_3 and w_3 one finds

$$J_{N_1} = \begin{pmatrix} -\sum_j \Gamma_j (|v_j|^2 + |w_j|^2) & 0 & 0 \\ 0 & \sum_j \Gamma_j |v_j|^2 & \sum_j \Gamma_j \overline{v_j} w_j \\ 0 & \sum_j \Gamma_j v_j \overline{w_j} & \sum_j \Gamma_j |w_j|^2 \end{pmatrix}. \quad (4.6)$$

With the usual Cartan subalgebra of diagonal matrices, there are two types of weight vector for the \mathbb{T}^2 action on $T_m M$, vectors with $w_j = 0$ (of weight $-\alpha_3$) and those with $v_j = 0$ (of weight α_2). Now N_1 consists of 4-dimension's worth of each. Eliminating v_3 and w_3 from the expression above, one finds, on the α_3 -weight space,

$$J_{N_1}(v_1, v_2, 0, 0) = \left(\frac{\Gamma_1}{\Gamma_3}(\Gamma_1 + \Gamma_3)|v_1|^2 + \frac{\Gamma_1 \Gamma_2}{\Gamma_3}(v_1 \overline{v_2} + \overline{v_1} v_2) + \frac{\Gamma_2}{\Gamma_3}(\Gamma_2 + \Gamma_3)|v_2|^2 \right) (-\alpha_3), \quad (4.7)$$

and on the α_2 -weight space,

$$J_{N_1}(0, 0, w_1, w_2) = \left(\frac{\Gamma_1}{\Gamma_3}(\Gamma_1 + \Gamma_3)|w_1|^2 + \frac{\Gamma_1 \Gamma_2}{\Gamma_3}(w_1 \overline{w_2} + \overline{w_1} w_2) + \frac{\Gamma_2}{\Gamma_3}(\Gamma_2 + \Gamma_3)|w_2|^2 \right) \alpha_2. \quad (4.8)$$

For both of these, using the notation of Lemma 4.3, one finds the discriminant

$$AC - B^2 = \frac{\Gamma_1 \Gamma_2}{\Gamma_3}(\Gamma_1 + \Gamma_2 + \Gamma_3). \quad (\mathbf{D})$$

This expression **(D)** is positive in regions A, B and D only. Consider the different cases:

(D) < 0: In this case the quadratic coefficients in (4.7) and (4.8) are indefinite, and the image of the momentum map at α contains lines in the root directions $\pm\alpha_2, \pm\alpha_3$, and in the positive Weyl chamber this gives lines in the directions $-\alpha_2$ and $-\alpha_3$. See for example Figure 4.3b. The convexity theorem implies that the infinitesimal momentum cone at α in this case contains the region between these two directions, but does not tell us if it is equal to it (see further below).

(D) > 0: Here there are two possibilities: the quadratic coefficients in (4.7) and (4.8) are either *positive* or *negative* definite. Suppose they are positive definite; then the image of J_{N_1} contains the directions α_2 and $-\alpha_3$. However, from α , the direction α_2 does not lie in the positive Weyl chamber, and applying the Weyl-group reflection fixing α sends α_2 to $-\alpha_3$. Thus all we know is that the image of J in a neighbourhood of α contains a line in the direction of $-\alpha_3$ (see Figures 4.2a and 4.2b). Similarly, if they are negative definite, the image contains a line in the direction of $-\alpha_2$ (as in Figure 4.2d).

Conclusion & construction of generic polytopes: For $\Gamma = (\Gamma_1, \Gamma_2, \Gamma_3)$ in each of the regions A, B, ..., H of the diagram in Figure 4.1, one plots the five points α (on the wall) and b, c_1, c_2, c_3 in the interior of the positive Weyl chamber. From each point, one can plot the local momentum cone. The theorem of Sjamaar (see Theorem 2.2(2) above) states,

$$\Delta(M) = \bigcap_{m \in \Phi^{-1}(\mathfrak{t}_+^*)} \Delta_m$$

where Δ_m is the local momentum cone at $\Phi(m)$ (independent of m in the fibre), as defined above. As can be seen from the figures, the points α, b and the c_j only account for some of the vertices (there may be others on the boundary of the Weyl chamber). However, if we put $\mathcal{V} = \{\alpha, b, c_1, c_2, c_3\}$, it follows from Sjamaar's theorem that

$$\Delta(M) \subset \bigcap_{\mu \in \mathcal{V}} \Delta_\mu. \quad (4.9)$$

In each region except G, the information from b, c_1, c_2, c_3 suffices. For example, for Γ in region D, refer to the weights shown in Figure 4.3a. Starting from the point c_1 , the weights dictate a line from c_1 to b , and from c_1 to c_3 to c_2 and thence to α . From b the weight in the direction α_2 leads to the wall. The convex hull of this set is the unique set satisfying the inclusion (4.9) and in addition containing the infinitesimal momentum cones (see Definition 2.1 and Theorem 2.2).

Region G: The argument above suffices for all the generic polytopes except those of region G; the three diagrams in Figure 4.4 are all compatible with the data at vertices b, c_1, c_2, c_3 , and we need to consider in greater detail the local momentum cone at α . This region G is defined by the inequalities $-\Gamma_3 > \Gamma_1 > \Gamma_2 > \Gamma_3$ and $\Gamma_1 + \Gamma_2 + \Gamma_3 > 0$ (see Figure 4.1), and hence expression (D) is negative. We need to determine in particular whether, at a point g of the line in the direction $-\alpha_3$ (see Figure 4.4), the infinitesimal momentum cone is the germ of a half space (above and to the right of the line, as in Figure 4.4a) or of the full space (as in Figures 4.4b, 4.4c).

To accomplish this, consider the point m' with $v_1 = 1, v_2 = w_1 = w_2 = 0$ in the symplectic slice N_1 at $m = (e_1, e_1, e_1)$; we have $J_{N_1}(m') = A(-\alpha_3)$, and put $g = \alpha + J_{N_1}(m')$. Here $A = (\Gamma_1 + \Gamma_3)\Gamma_1/\Gamma_3 < 0$ in region G. (One could replace $v_1 = 1$ with $v_1 = \epsilon$ to ensure g

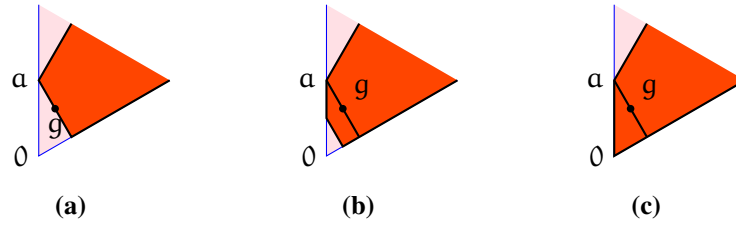


Figure 4.4: Three possibilities for the lower part of polytope G compatible with local information at vertices b, c_1, c_2, c_3 —version (a) is the correct one as shown by considering the local momentum cone at g .

is in the positive Weyl chamber, but the calculation is identical save for a factor of ϵ^2 .) Let us calculate the infinitesimal momentum cone δ' at this point. For the $U(2)$ action on N_1 , the point m' has stabilizer $U(1)$ generated by $\text{diag}[i, i, -2i] \in \alpha_3^\circ$ (cf. Lemma 2.3). Moreover $G_g = \mathbb{T}^2$. Considering the $U(2)$ -action on N_1 gives rise to a Witt-Artin decomposition at m' given by

$$T_{m'}(N_1) = T'_0 \oplus T'_1 \oplus N'_1 \oplus N'_0$$

with $\dim T'_0 = \dim N'_0 = 1, \dim T'_1 = 2$ leaving $\dim N'_1 = 4$. Now, a local calculation shows that

$$N'_1 = \{(v_1, v_2, w_1, w_2) \in N_1 \mid Av_1 + Bv_2 = Aw_1 + Bw_2 = 0\},$$

where A, B are as before the coefficients in (4.7) above. This space can be parametrized by $v_1 = v, w_1 = w$ and hence $v_2 = -(A/B)v, w_2 = -(A/B)w$. The image of N'_0 under the momentum map is the line along the root direction $\pm\alpha_3$. Moreover so is the image of $(v, 0)$. Indeed, the $U(2)$ -momentum map on N'_1 is

$$J_{N'_1}(v, w) = \frac{A}{B^2}(AC - B^2) \begin{pmatrix} -|v|^2 - |w|^2 & 0 & 0 \\ 0 & |v|^2 & \bar{v}w \\ 0 & v\bar{w} & |w|^2 \end{pmatrix}.$$

This lies in \mathfrak{t}^* if and only if $\bar{v}w = 0$. The case $(v, 0)$ has been mentioned, leaving the case $(0, w)$:

$$J_{N'_1}(0, w) = \frac{A}{B^2}(AC - B^2)|w|^2 \text{diag}[-1, 0, 1] = \frac{A}{B^2}(AC - B^2)|w|^2 \alpha_2.$$

Now, in region G , the coefficient $(A/B^2)(AC - B^2) < 0$, and since the infinitesimal momentum cone δ' is independent of the point in the fibre (Theorem 2.2), this shows that the infinitesimal momentum cone is indeed the half space as claimed.

With this the proof of Theorem 4.1 is concluded. \square

4.2 Transition polytopes

The 8 regions of the Γ -plane (Figure 4.1) are separated by ‘transition cases’, such as occur when $\Gamma_1 = \pm\Gamma_2$ or $\Gamma_1 = \Gamma_2 + \Gamma_3$. There are also the possibilities of $\Gamma_j = 0$, but these we are excluding from consideration as the polytope coincides with that of the 2 point polytopes described in

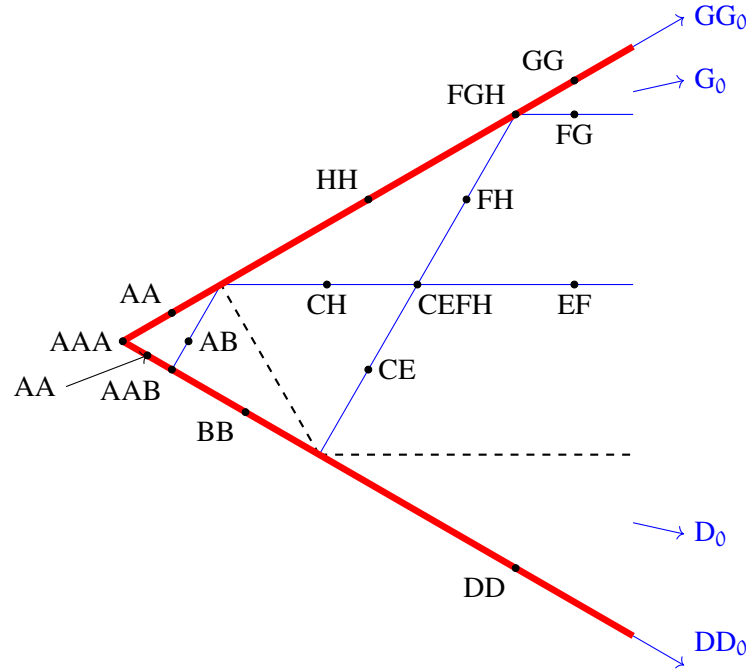


Figure 4.5: This shows the labels of all 20 transition polytopes with $\Gamma_j \neq 0$. Compare with Fig. 4.1. The transitions denoted D_0 , DD_0 , G_0 and GG_0 arise ‘at infinity’ in this diagram, and refer to points with $\Gamma_1 + \Gamma_2 + \Gamma_3 = 0$; the polytopes are illustrated in Figure 4.7. The transition between D_0 and G_0 occurs when $\Gamma_2 = \Gamma_1 + \Gamma_3 = 0$.

Section 3. At each of these transitions, one of the vertices of the polytope hits a wall of the Weyl chamber, and a different analysis of the weights is required; indeed the dimension of the symplectic slice is no longer the same. It can also happen that two of the vertices coincide (such as $c_2 = c_3$ when $\Gamma_2 = \Gamma_3$ in the transitions denoted BB and DD), but this does not effect the weight calculations, which are local in M . The transition polytopes are illustrated in Figures 4.8 and 4.9; the notation for the different transition cases are shown in Figure 4.5.

However, rather than repeating the weight calculations, it is sufficient to use a continuity argument. Since M (and hence M/G) is compact, and the momentum map depends continuously on Γ , it follows that the image of the orbit momentum map \mathcal{J} also depends continuously on Γ . It suffices therefore to follow the movement of the vertices as one approaches the boundary of any particular region to conclude the shape of each of the transition momentum polytopes.

In Figure 4.6 one sees the transition between a polytope of Type A and one of Type B, through the intermediate AB (which occurs when $\Gamma_1 = \Gamma_2 + \Gamma_3$, assuming as always that $\Gamma_1 \geq \Gamma_2 \geq \Gamma_3$). In region B, the point c_1 is the image under J of $m = (e_1, e_2, e_2)$. As the Γ_j are varied towards region A, the point $J(m)$ moves towards the boundary of the positive Weyl chamber, and crosses the wall so that in region A the point $J(m)$ is no longer in the positive Weyl chamber. In region A, the point c_1 is the value $J(m')$ for $m' = (e_2, e_1, e_1)$. At the transition (Type AB), both of these points map to the same point in the wall of \mathfrak{t}_+^* . Note that in general, the two values

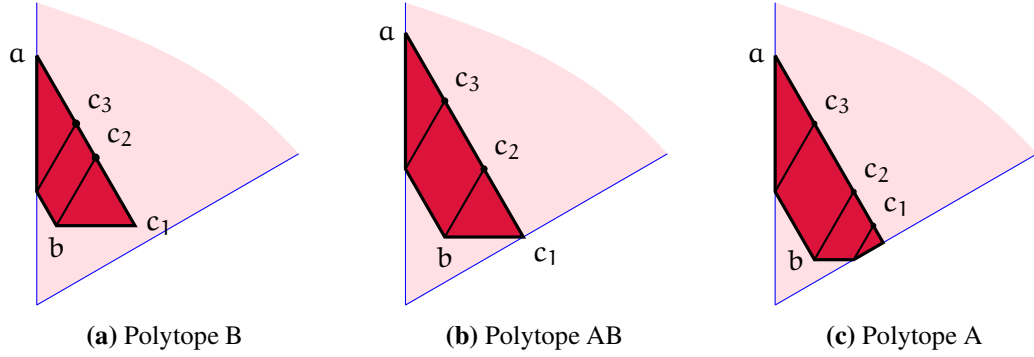


Figure 4.6: This shows the transition $B \rightarrow AB \rightarrow A$, involving vertex c_1 moving to the boundary of the Weyl chamber and getting reflected back but leaving an edge ‘stuck’ to the boundary. See text for further explanation.

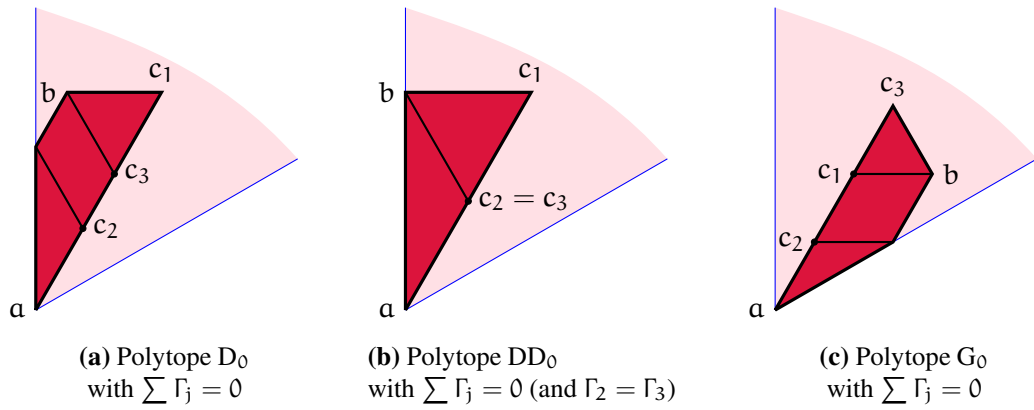


Figure 4.7: Polytopes arising for $\Gamma_1 + \Gamma_2 + \Gamma_3 = 0$, which implies $a = 0$. Notice that D_0 and G_0 are related by a reflection in the centre line of the Weyl chamber; this is because reversing the signs of the Γ_j converts region G_0 to D_0 , via the involution $*$ described in Remark 2.4. A similar observation relates the polytopes for DD_0 and GG_0 (the latter not drawn). See Figure 4.5 for the regions in parameter space.

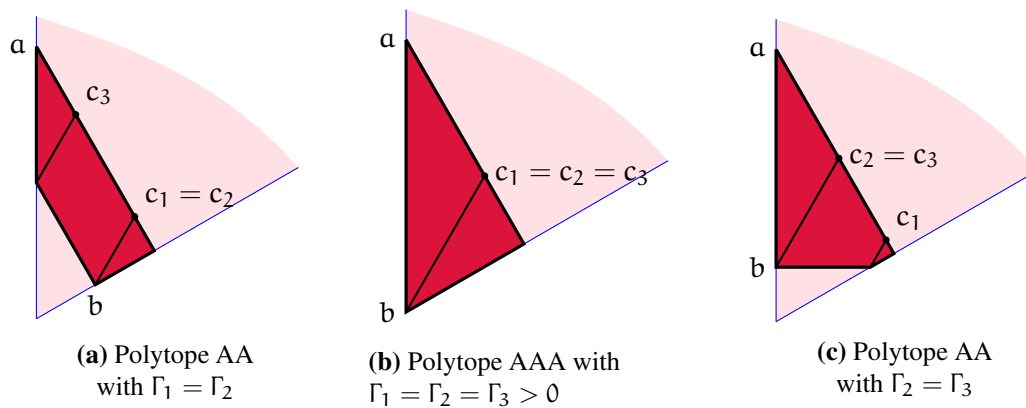


Figure 4.8: The transition polytopes with repeated weights around region A.

$J(m)$ and $J(m')$ have the same spectrum and are related by an element of the Weyl group.

Symplectic reduction In the companion paper [10], we describe the reduced spaces M_μ for $\mu \in \Delta(M)$. The possibilities for M_μ are a sphere, a sphere with singularities and a single point.

References

- [1] M.F. Atiyah, Convexity and commuting Hamiltonians, *Bull. London Math. Soc.* **14**, (1982), no. 1, 1-15.
- [2] L. Bedulli & A. Gori, On deformations of Hamiltonian actions. *Arch. Math.* **88** (2007), 468–480.
- [3] V. Guillemin & S. Sternberg, Convexity properties of the moment mapping, *Invent. Math.* **67** (1982), no. 3, 491-513.
- [4] V. Guillemin & S. Sternberg, *Symplectic Techniques in Physics*. CUP, 1984.
- [5] A. Horn, Doubly stochastic matrices and the diagonal of a rotation matrix, *Amer. J. Math.* **76** (1954), 620–630.
- [6] F.C. Kirwan, Convexity Properties of the Moment Mapping III, *Invent. Math.* **77** (1984), 547–552.
- [7] A. Knutson, The symplectic and algebraic geometry of Horn’s problem. *Linear Alg. Appl.* **319** (2000), 61–81.
- [8] B. Kostant, On convexity, the Weyl group and the Iwasawa decomposition, *Ann. Sci. Ecole Norm. Sup., Série 4* **6** (1973), 413–455.
- [9] J. Montaldi & M. Roberts, Stratification of the momentum map. *In preparation* (2019).
- [10] J. Montaldi & A. Shaddad, Generalized point vortex dynamics on \mathbb{CP}^2 . *J. Geom. Mechanics* (2019) (to appear).
- [11] J. Montaldi & T. Tokieda, Openness of momentum maps and persistence of extremal relative equilibria. *Topology* **42** (2003), 833–844.
- [12] J.-P. Ortega and T.S. Ratiu, *Momentum Maps and Hamiltonian Reduction*, Springer, 2004.

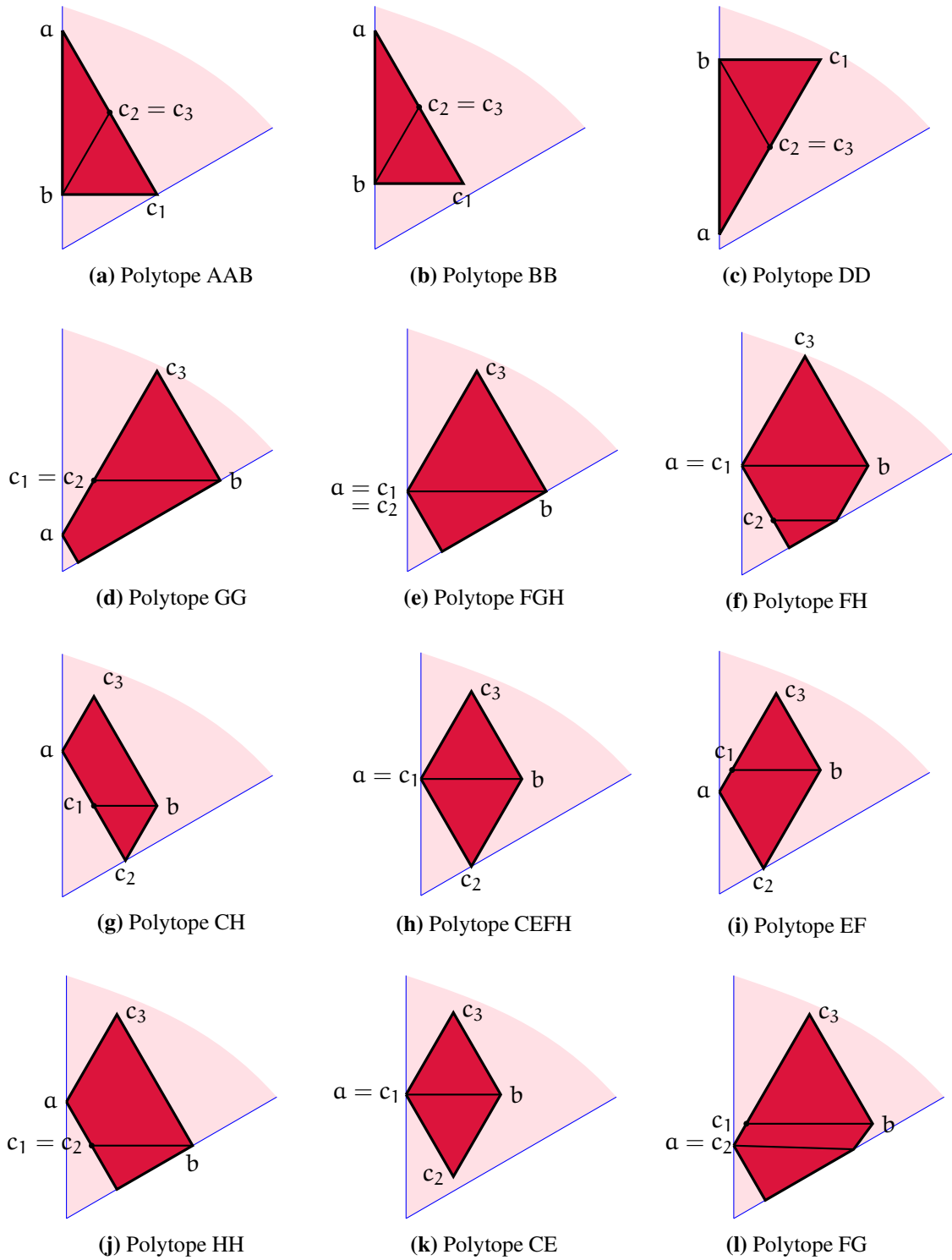


Figure 4.9: The remaining transition polytopes—see Fig. 4.5 for notation

- [13] I. Schur, Über eine Klasse von Mittelbildungen mit Anwendungen auf der Determinantentheorie (On a class of averaging with application to the theory of determinants), *Sitzungsberichte der Berliner Mathematischen Gesellschaft*, **22** (1923), 9-20.
- [14] A. Shaddad, *The classification and dynamics of the momentum polytopes of the $SU(3)$ action on points in the complex projective plane with an application to point vortices*. Ph.D. thesis, University of Manchester, 2018.
- [15] R. Sjamaar, Convexity properties of the moment mapping re-examined. *Advances in Math.* **138** (1998), 46–91.

JM: j.montaldi@manchester.ac.uk

AS: amna.shaddad@gmail.com

School of Mathematics

University of Manchester

Manchester M13 9PL, UK